



Supplement of

Wintertime aerosol chemistry and haze evolution in an extremely polluted city of the North China Plain: significant contribution from coal and biomass combustion

Haiyan Li et al.

Correspondence to: Qiang Zhang (qiangzhang@tsinghua.edu.cn) and Kebin He (hekb@tsinghua.edu.cn)

The copyright of individual parts of the supplement might differ from the CC-BY 3.0 licence.

23 **Section S1. Analysis to determine the best solution for ME-2**

24 Using the multi-linear engine (ME-2) implemented with the toolkit SoFi (Source Finder), organic
25 source apportionment was performed with the so-called a value approach. The a value determines the
26 extent to which the resolved factor profiles ($f_{j,solution}$) or time series ($g_{i,solution}$) are allowed to vary from the
27 input ones (f_j , g_i) (Canonaco et al., 2013):

28 $f_{j,solution} = f_j \pm a \cdot f_j,$

29 $g_{i,solution} = g_i \pm a \cdot g_i,$

30 To separate an individual HOA factor in addition to CCOA, BBOA and OOA, we only constrained
31 the mass spectra of HOA in this study, using the reference profile from Ng et al. (2011). Some important
32 criterions to select the optimal solution with a value varying from 0 to 1 are shown in Fig. S2-S6.
33 Generally, increasing a value decreases Q and the ratio of Q to Q_{exp} , due to additional degrees of freedom.
34 However, the size of the change of Q/ Q_{exp} over different a values is not significant (Fig. S2a). In addition,
35 the explained variation (EV) could indicate how much variation in each variable is explained by each
36 factor. According to Paatero (2004), a variable should be considered only if the unexplained EV for that
37 variable is less than 25% (Fig. S2c).

38 Combining the analysis of factor profiles and time series of each factor across different a values,
39 there is no significant variations for CCOA and OOA. By contrast, with different constraint levels, large
40 changes were found for HOA and BBOA, which were mixed during PMF analysis. As shown in Fig. S3a,
41 moving from a constrained run to a less constrained situation apportioned more signals to larger m/z for
42 HOA profile. For a values from 0.2 to 1.0, fractions of m/z smaller than 50 for BBOA profile were
43 significantly enhanced and the time series of BBOA were similar to those of OOA. These results
44 indicated that solutions for a value of 0 and 0.1 were more reasonable. This was further evidenced by the
45 diurnal profiles of each factor and their correlations with external tracers over different a values. To allow
46 some degrees of freedom for model run, we chose the results for a value of 0.1 to be the best solution in
47 this study.

Table S1. Summary of online measurements ($\mu\text{g}/\text{m}^3$) using an Aerodyne ACSM or AMS during wintertime in China.

Sampling site	Handan, Hebei	Beijing	Beijing	Beijing	Beijing	Lanzhou, Gansu	Nanjing, Jiangsu	Jiaxing, Zhejiang	Ziyang, Sichuan
Location	36.57°N, 114.50°E	39.99°N, 116.31°E	39.97°N, 116.37°E	39.97°N, 116.37°E	39.97°N, 116.37°E	36.05°N, 103.85°E,	32.05°N, 118.77°E	30.8°N, 120.8°E	30.15°N, 104.64°E
Period	Dec.3,2015- Feb.5, 2016	Nov.22- Dec.22, 2010	Nov.21,2011- Jan.20,2012	Jan.1- Feb.1,2013	Dec.17,2013- Jan.17,2014	Jan.10- Feb.4,2014	Dec.1-31, 2013	Dec.11-23, 2010	Dec.3,2012- Jan.5,2013
instrument	ACSM ^a	HR-AMS ^b	ACSM	HR-AMS	HR-AMS	HR-AMS	ACSM	HR-AMS	HR-AMS
NR-PM ₁	173.4	63.5	66.2	89.2	63.9	53.6	90.2	34.9	52.9
Sulfate	28.1	8.7	9.3	19.6	9.6	7.2	14.3	7.1	12.2
Nitrate	26.1	6.8	10.6	12.5	7	9.5	22.3	7.5	8.9
Ammonium	21.4	7.7	8.6	8.9	5.1	5.9	12.5	4.9	8.2
Chloride	16.6	5.8	3.3	3.6	3.8	1.7	2.7	2.7	2.1
Organic	81.2	34.5	34.4	44.6	38.4	29.3	38.4	12.7	21.5
HOA	6	4.7	5.8	4.9	3.8	2.6	5	5	3.2
COA	N.D. ^c	6.7	6.5	8.9	6.9	5.8	5	N.D.	N.D.
BBOA	20.7	4.1	N.D.	N.D.	3.3	3.2	5.8	3.8	3

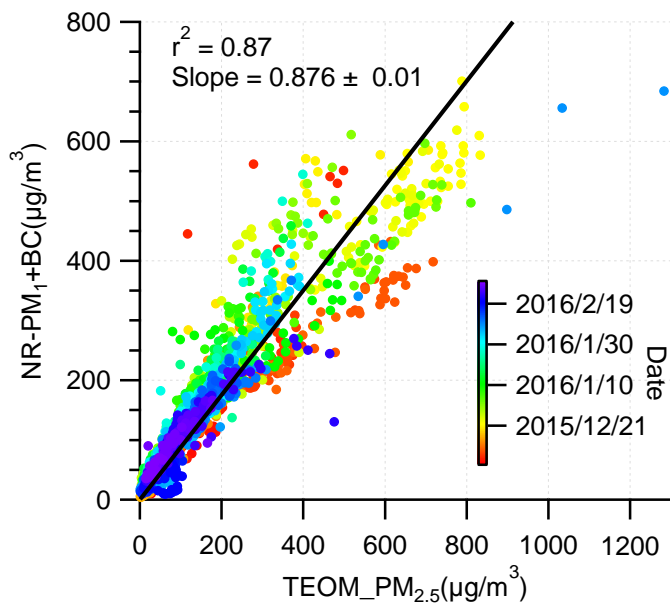
CCOA	23.1	8.2	11.4	6.7	7.6	5.3	N.D.	N.D.	N.D.
OOA	31.4	N.D.	10.7	N.D.	16.9	N.D.	N.D.	3.8	N.D.
SV-OOA	N.D.	N.D.	N.D.	11.6	N.D.	7	N.D.	N.D.	7.8
LV-OOA	N.D.	N.D.	N.D.	12.5	N.D.	5.6	8.8	N.D.	7.5
LO-OOA	N.D.	4.3	N.D.	N.D.	N.D.	N.D.	4.6	N.D.	N.D.
MO-OOA	N.D.	6.2	N.D.	N.D.	N.D.	N.D.	9.2	N.D.	N.D.
Reference		Hu et al. this study	Sun et al. (2013)	Zhang et al. (2014)	Sun et al. (2016)	Xu et al. (2016)	Zhang et al. (2015)	Huang et al. (2012)	Hu et al. (2016b)

49 ^aAerosol Chemical Speciation Monitor (ACSM)

50 ^b High Resolution Time-of-Flight Aerosol Mass Spectrometer (HR-AMS)

51 ^c N.D. = not detected.

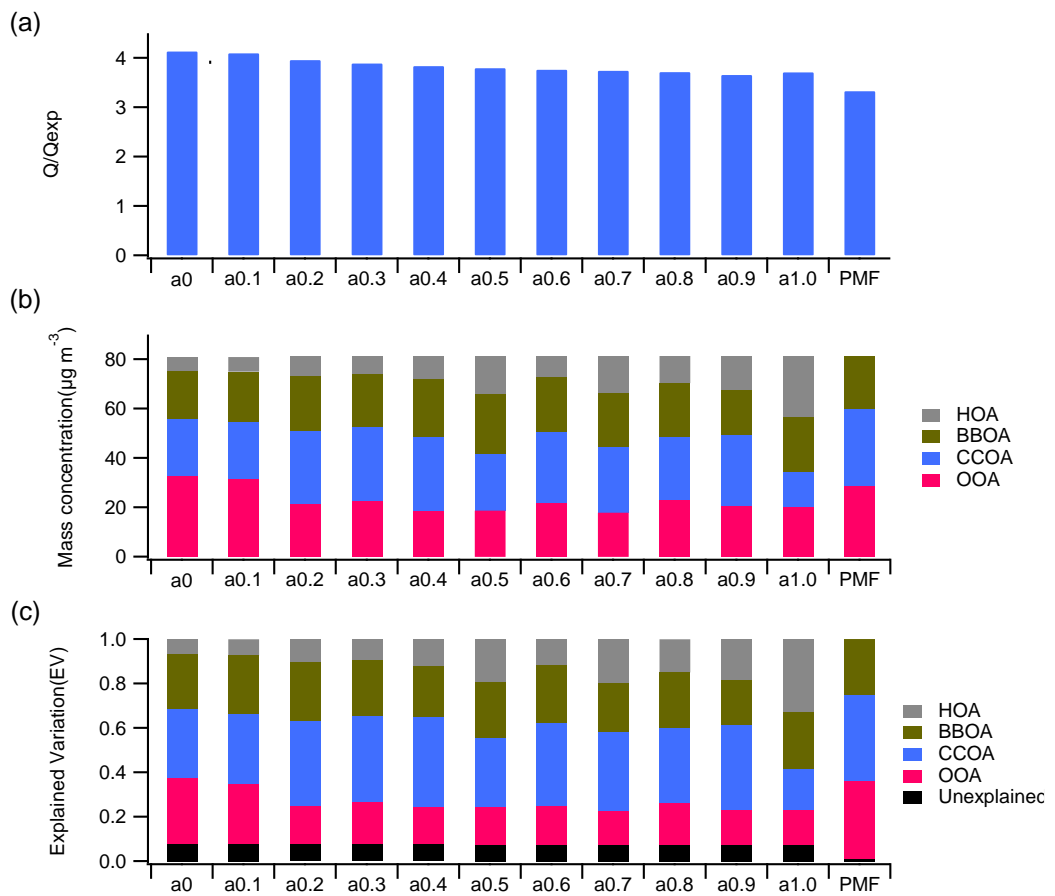
52



53

54 **Figure S1.** Correlation of NR-PM₁ measured by ACSM plus BC measured by MAAP with PM_{2.5} measured by
 55 TEOM.

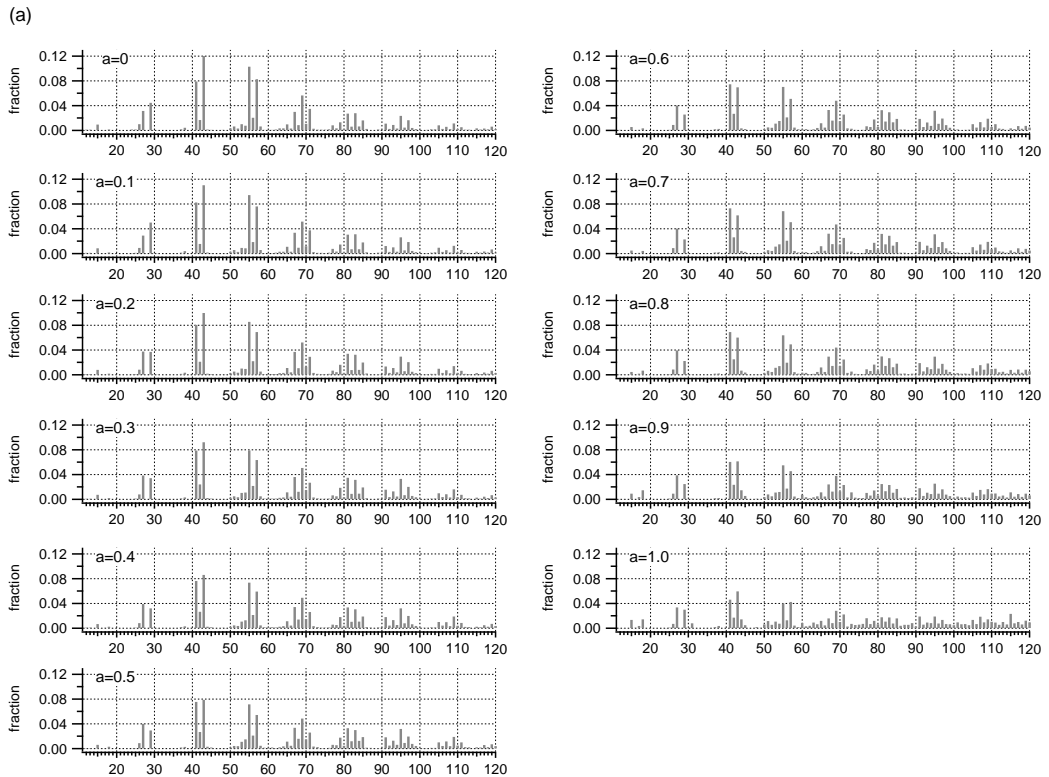
56



57

58 **Figure S2.** (a) Values of Q/Qexp, (b) mass concentrations of each factor and (c) explained variation (EV) for
59 each factor and total unexplained variation (UEV) for different model runs. The PMF result shown here is for 3-
60 factor solution.

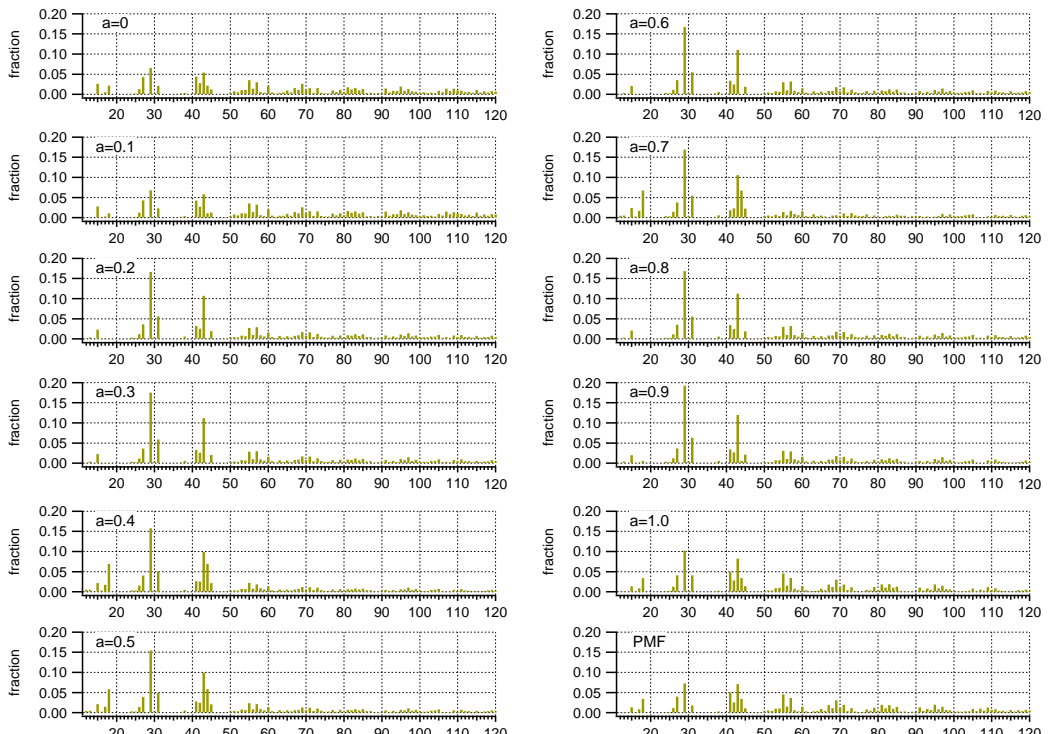
61



62

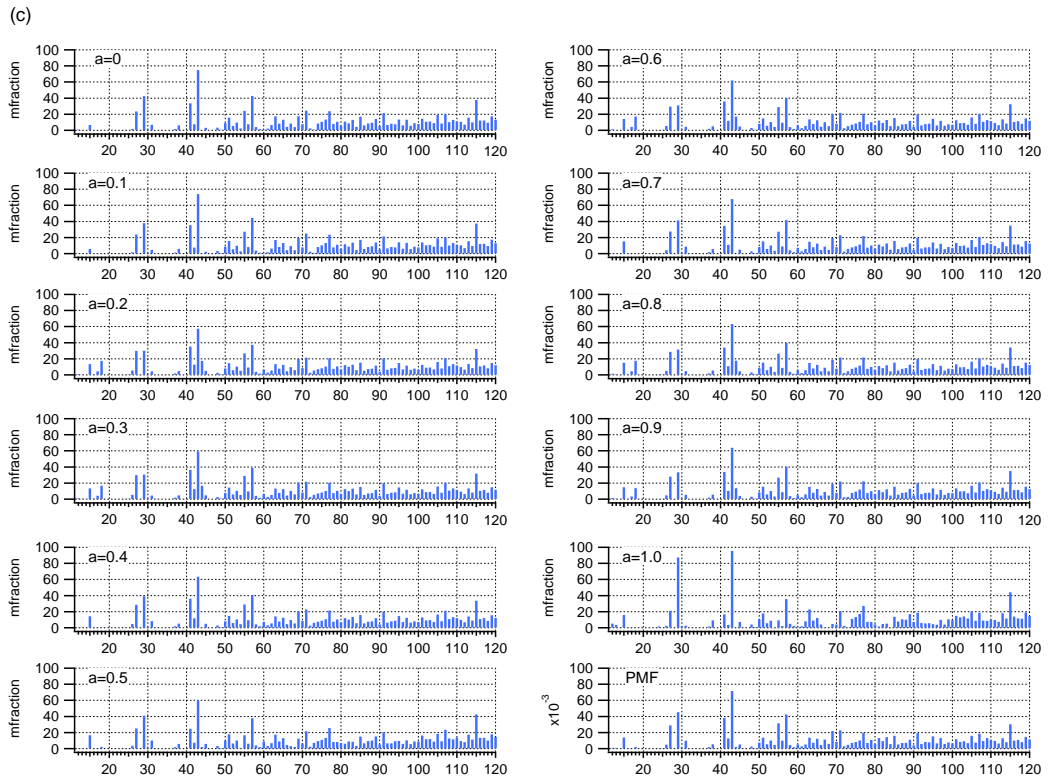
63

(b)



64

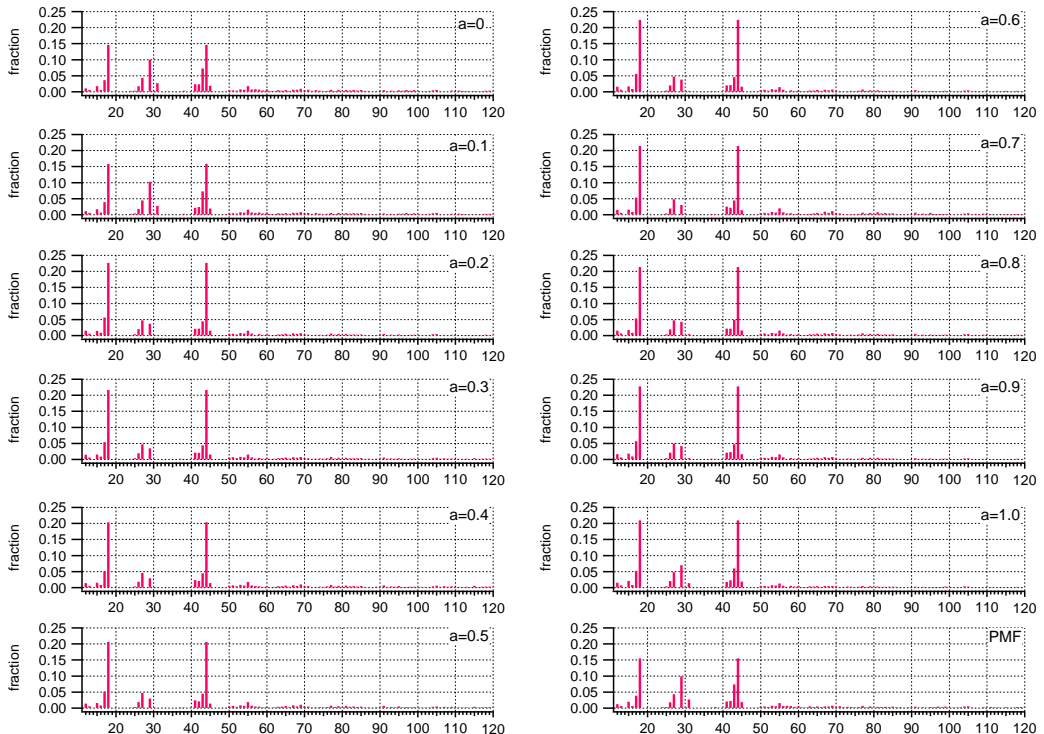
65



66

67

(d)

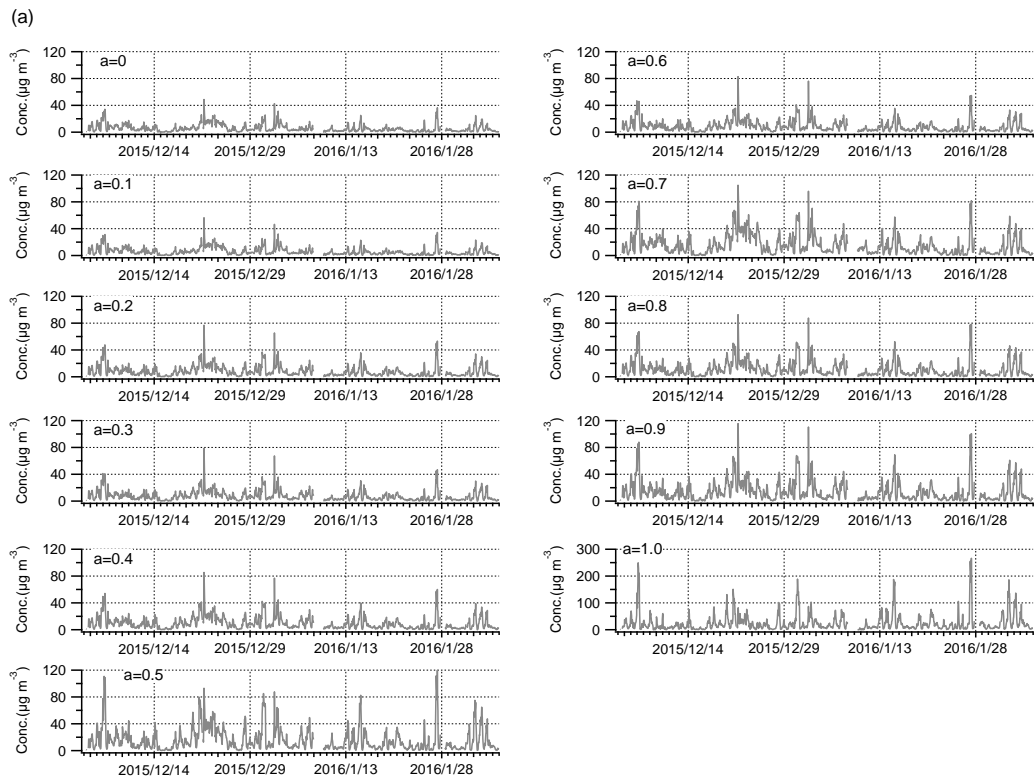


68

69

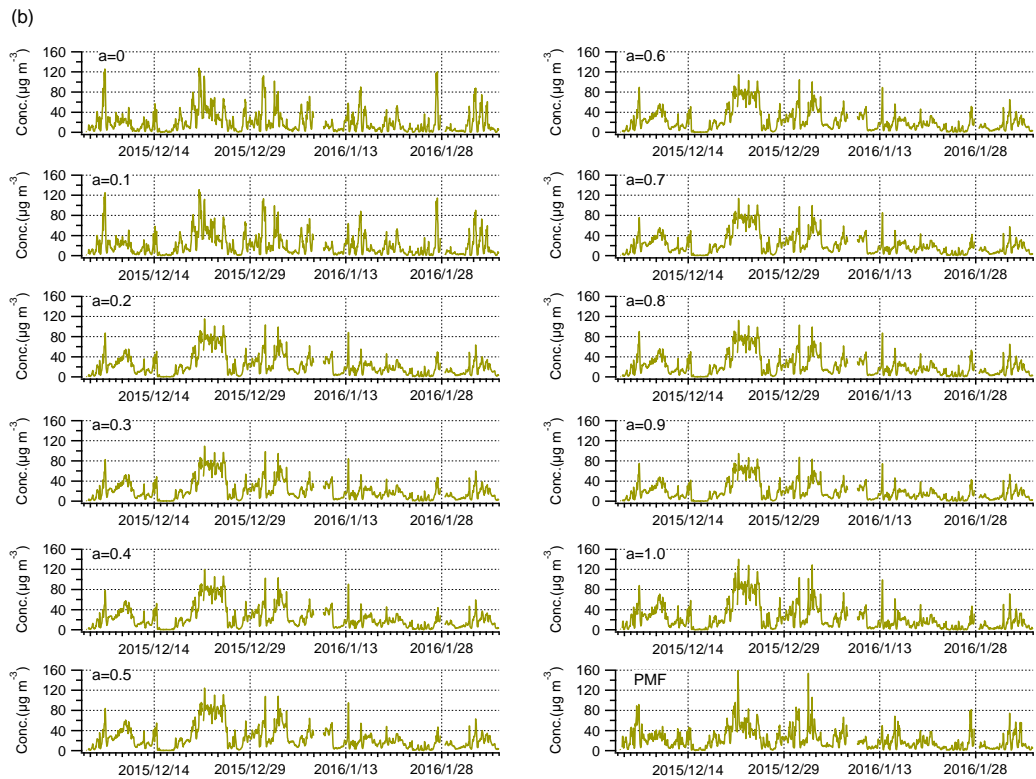
Figure S3. Factor profiles of (a) HOA, (b) BBOA, (c) CCOA and (d) OOA for different model runs

70



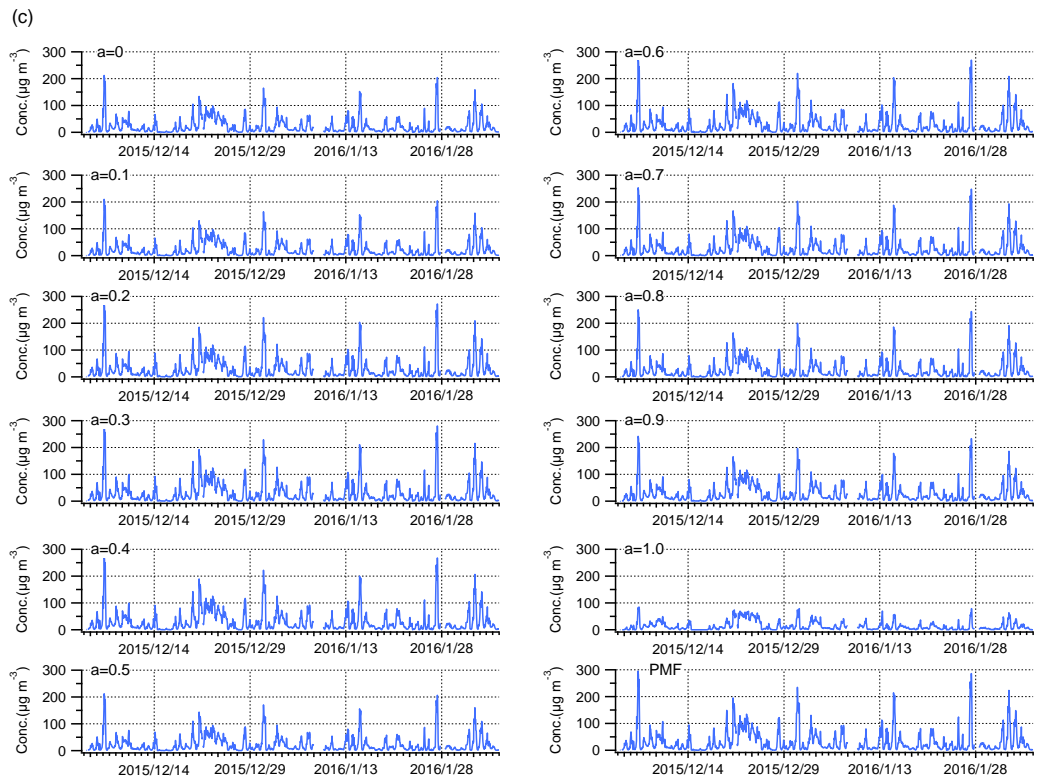
71

72



73

74



75

76

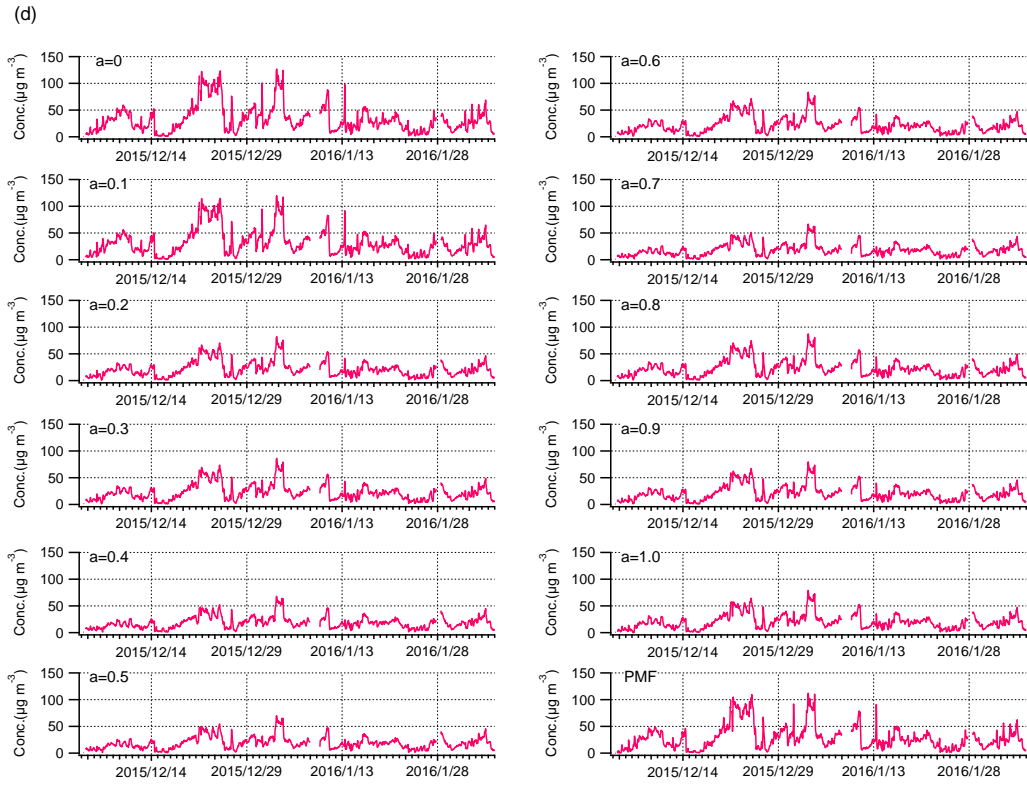
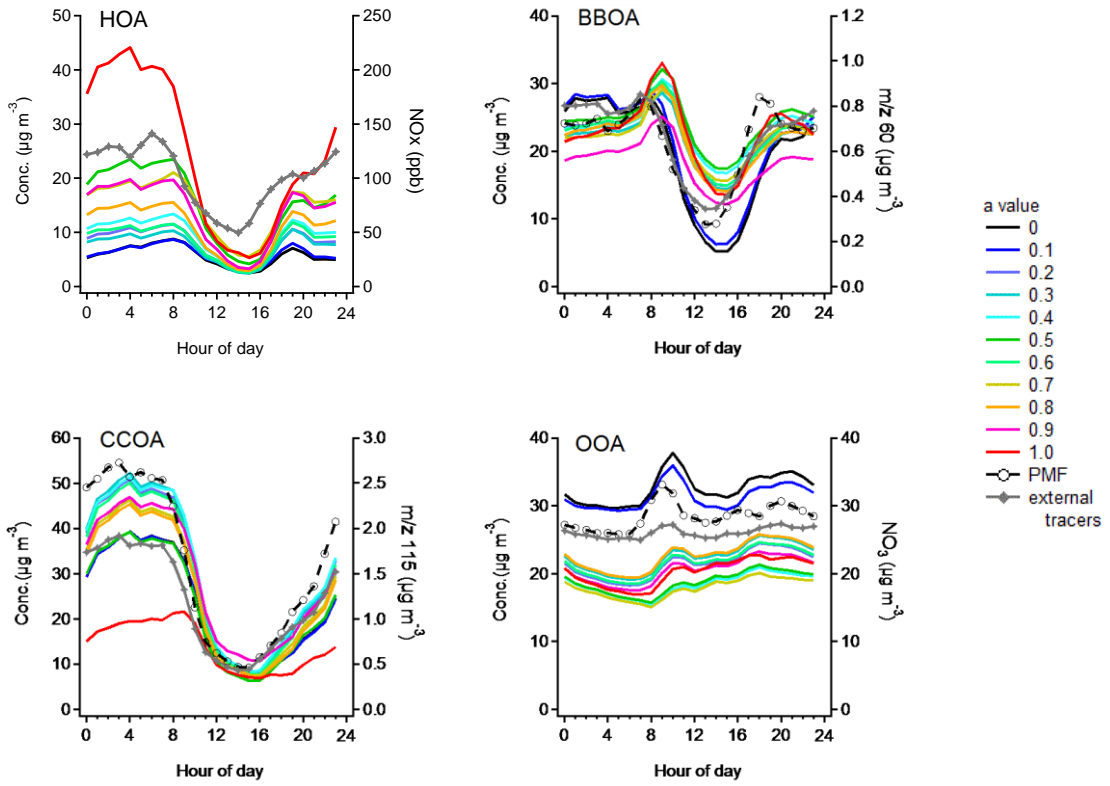


Figure S4. Time series of (a) HOA, (b) BBOA, (c) CCOA and (d) OOA for different model runs.

77
78

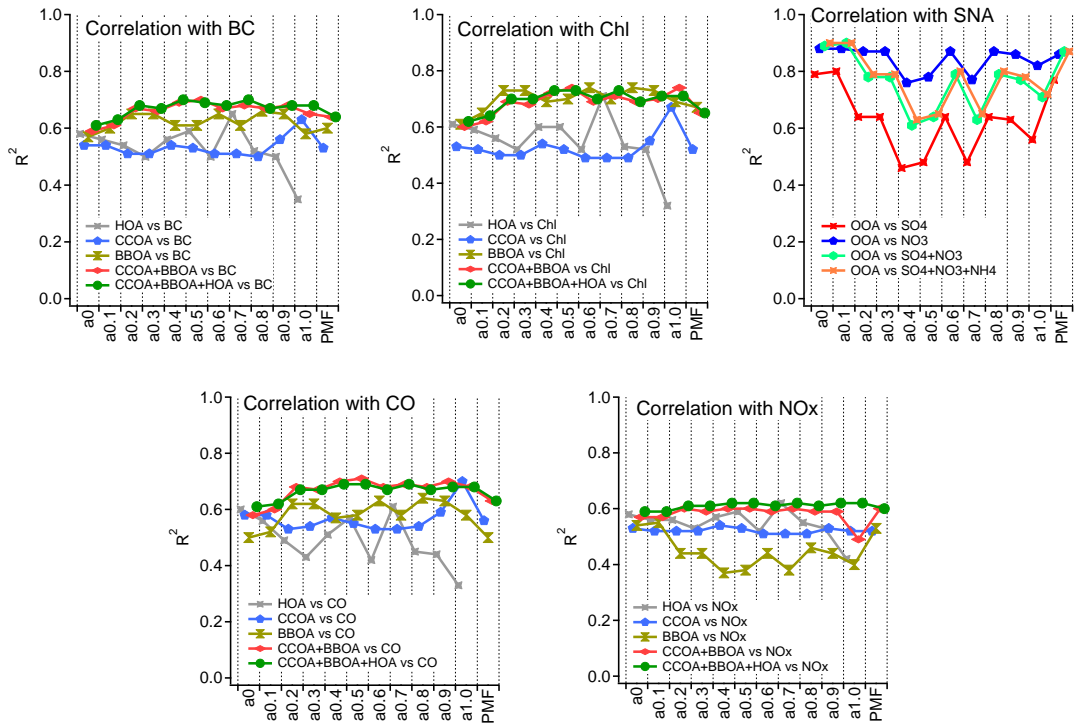
79



80

81 **Figure S5.** Mean diurnal variations of HOA, BBOA, CCOA and OOA for different model runs, with the
 82 variations of their external tracers on the right axis.

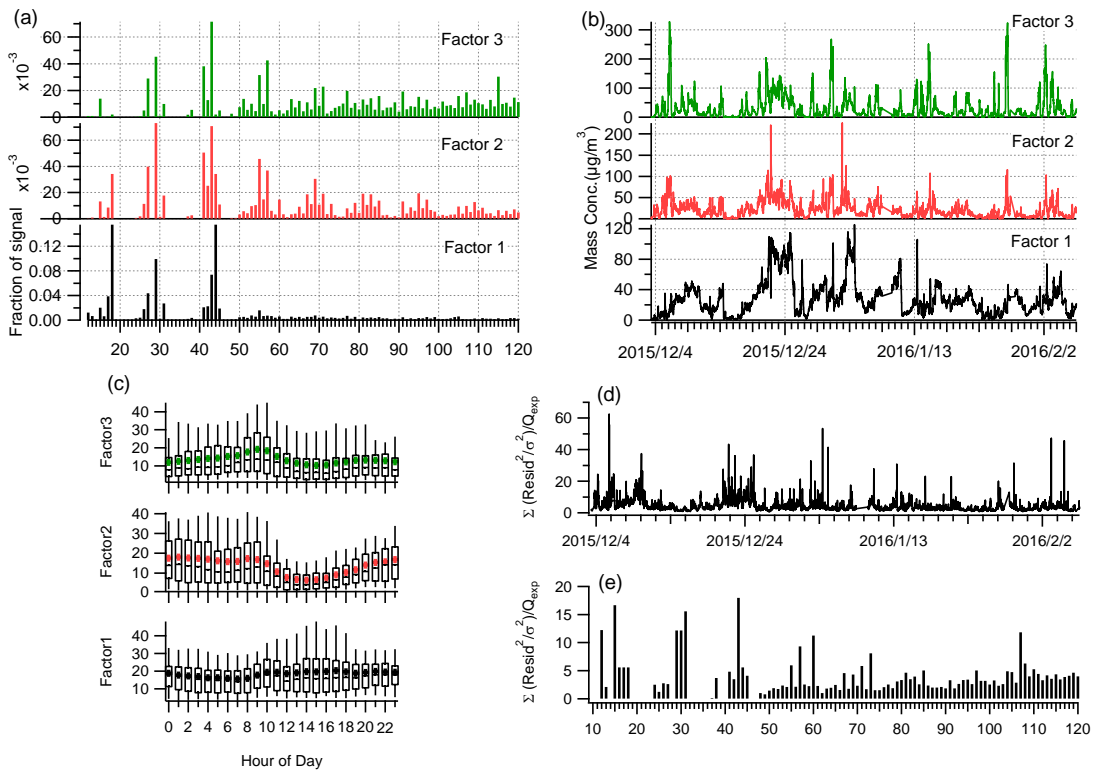
83



84

85 **Figure S6.** Correlations R^2 (Pearson) between the time series of OA factors and the time series of external
86 tracers as a function of model runs.

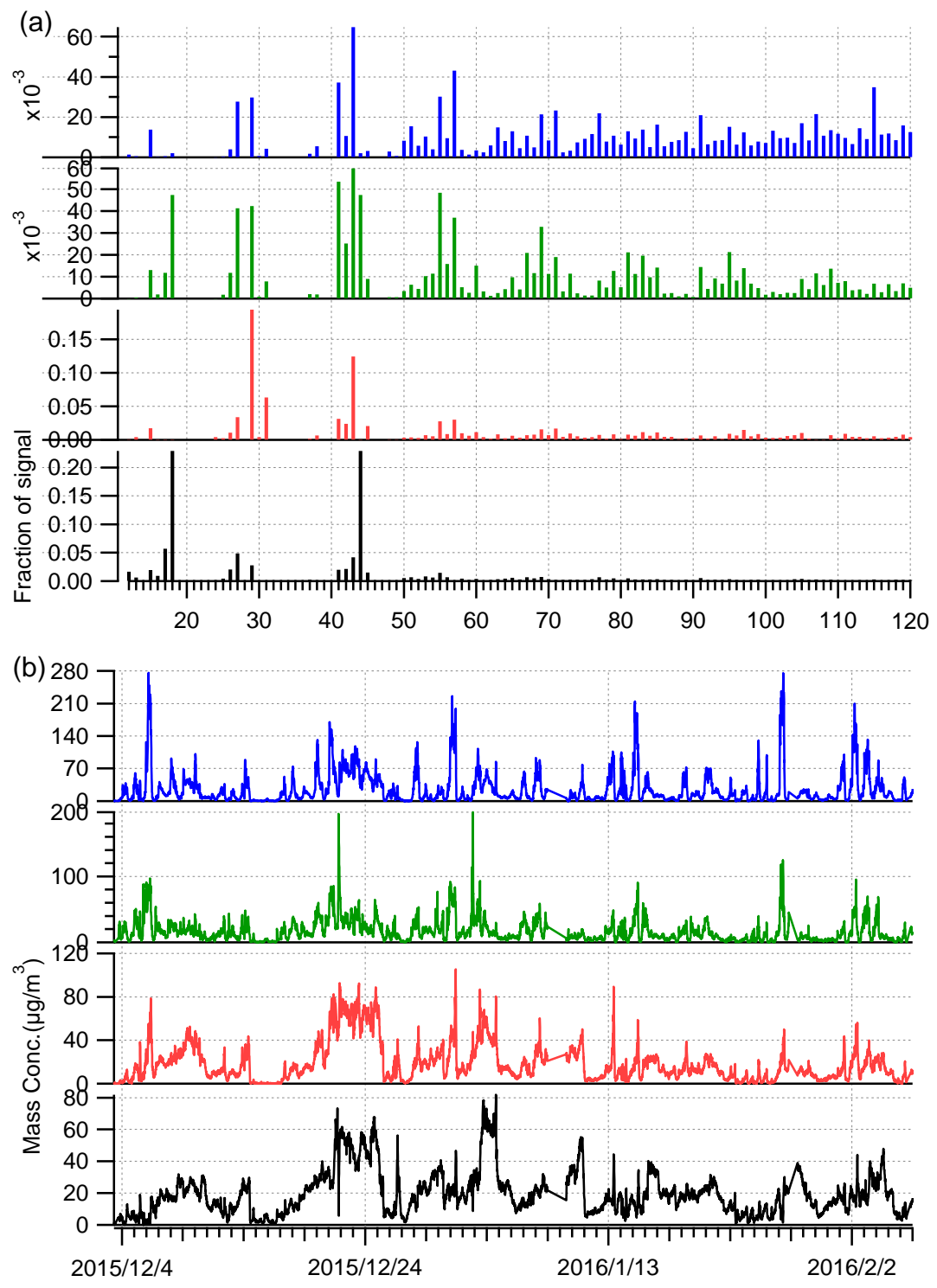
87



88

Figure S7. (a) Spectral profiles, (b) time series, (c) diurnal patterns, (d) time series of Q/Qexp, and (e) spectral profile of Q/Qexp for 3-factor solution of PMF analysis.

91

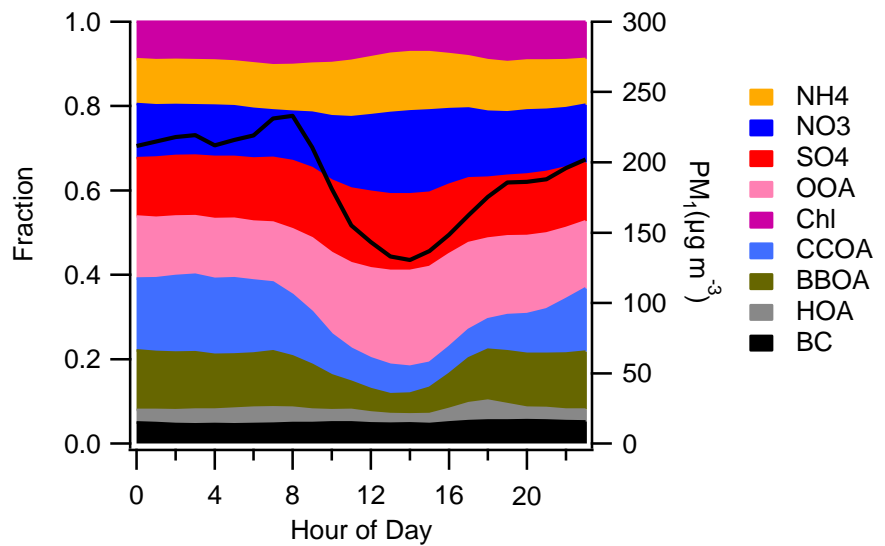


92

93

Figure S8. (a) Spectral profiles and (b) time series for 4-factor solution of PMF analysis.

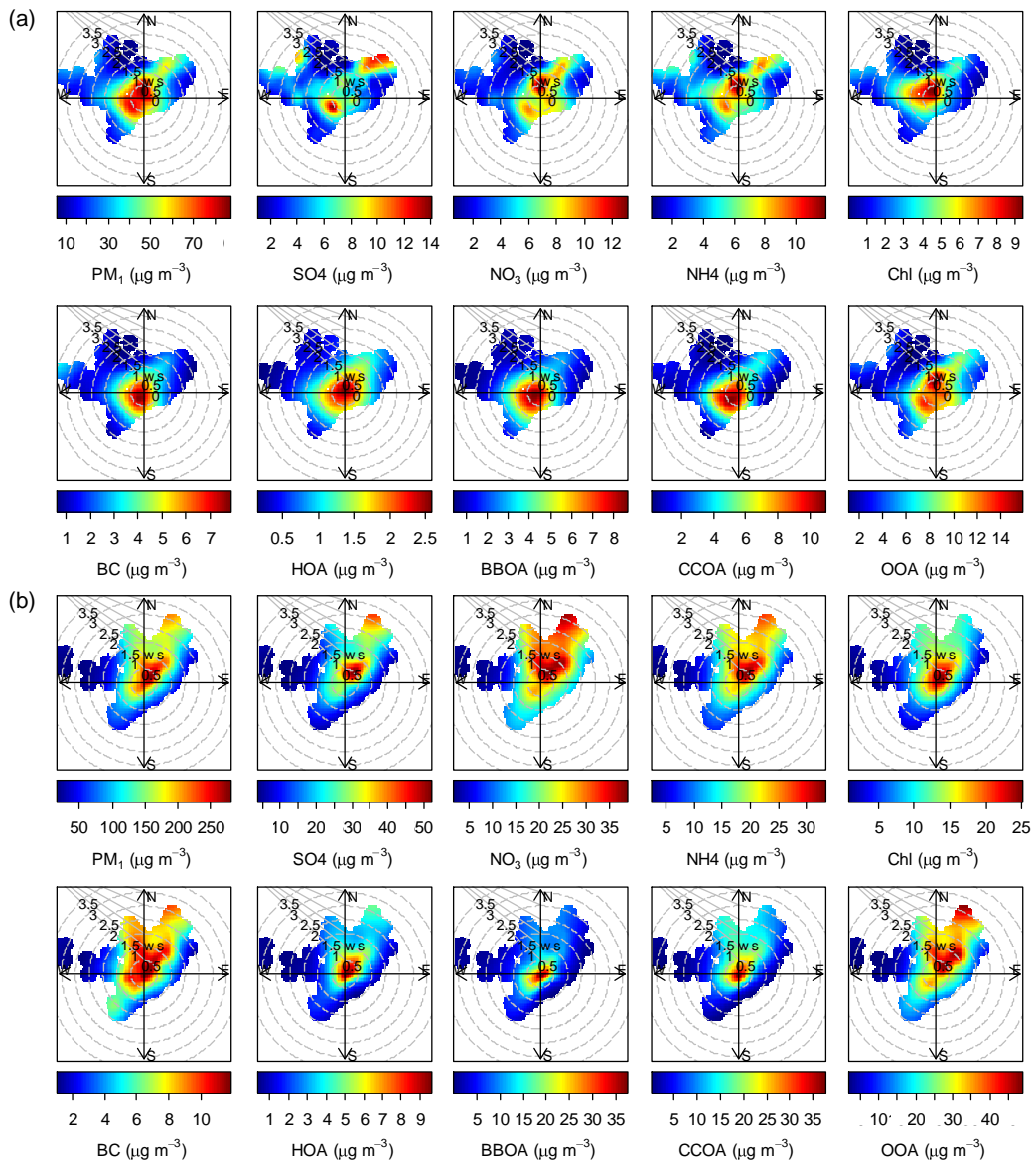
94



95

96

Figure S9. Average diurnal cycles of the mass fractions of aerosol species.

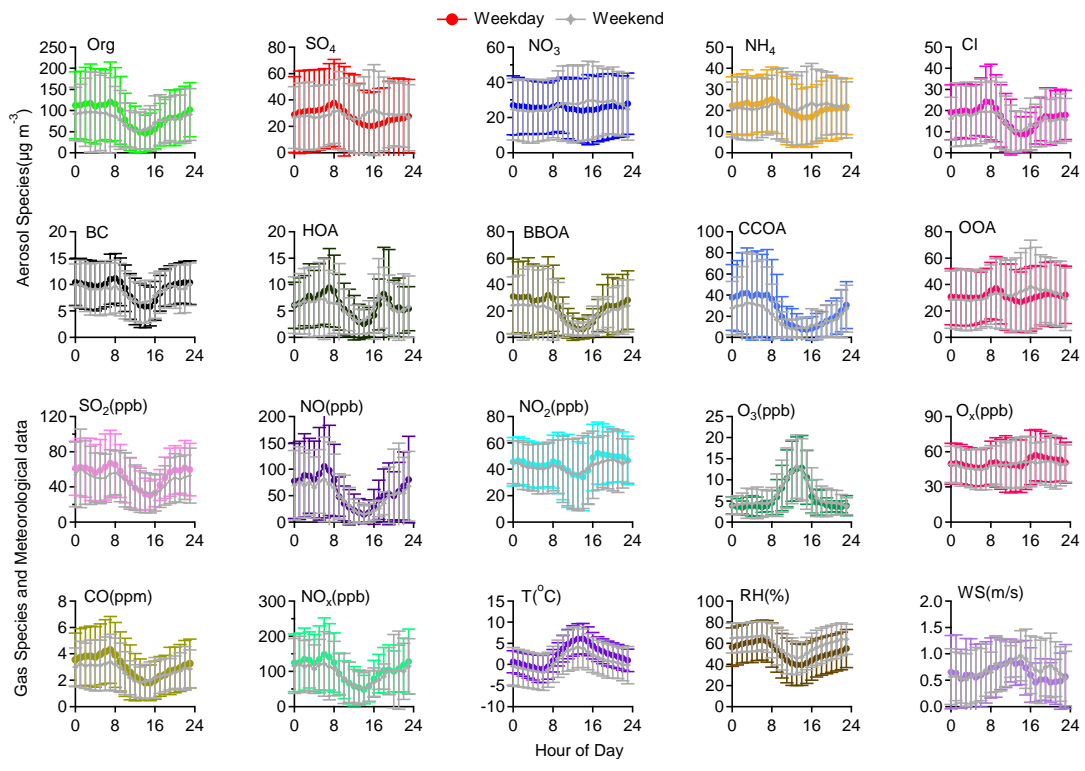


97

98

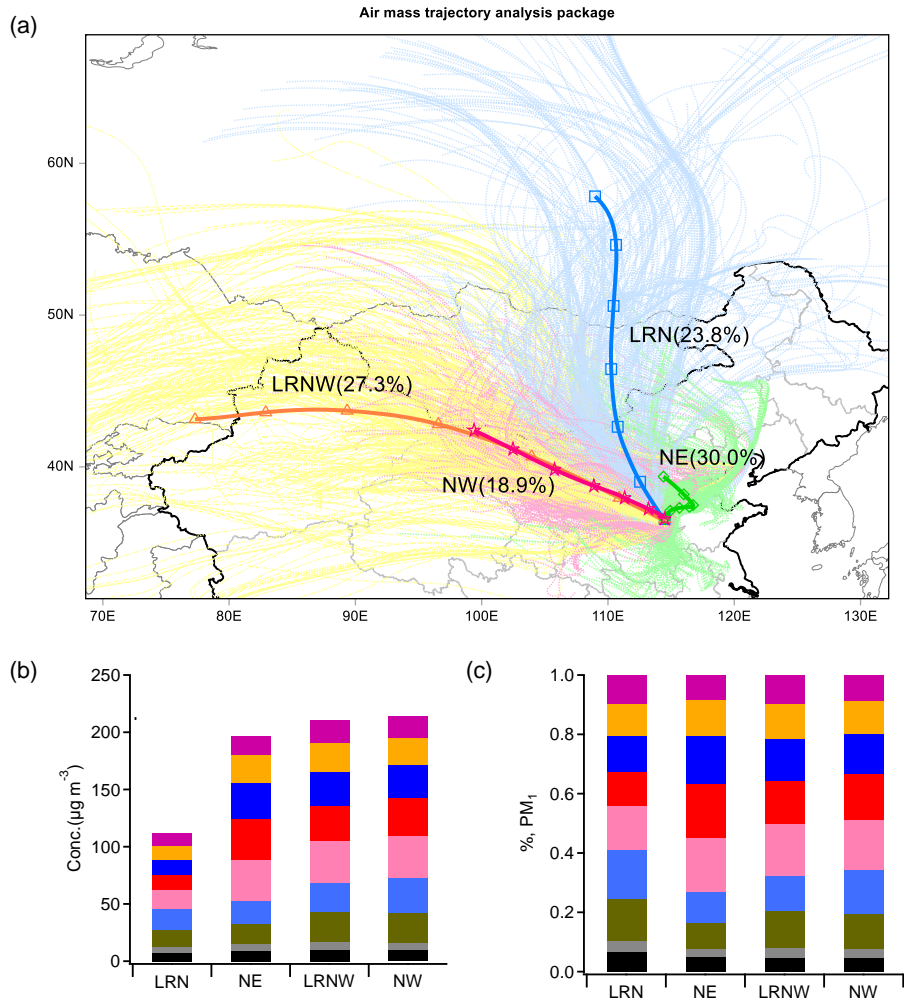
Figure S10. Polar plots of aerosol components as a function of wind speed and wind direction for (a) non-polluted and (b) polluted periods.

99



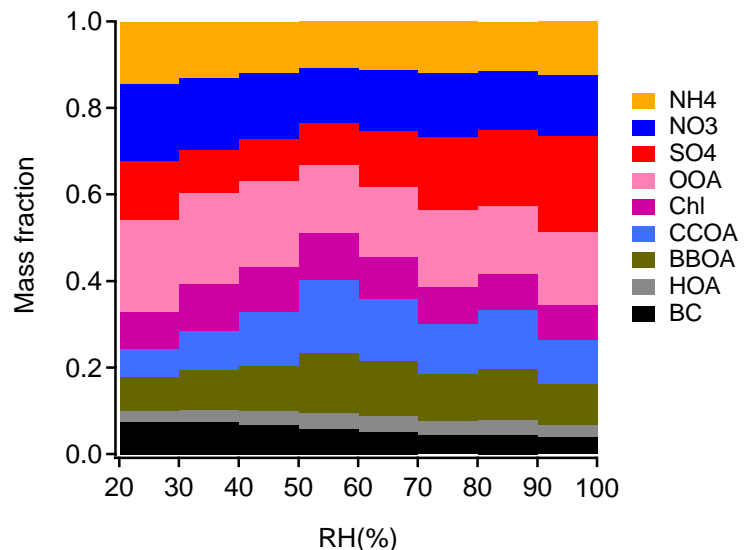
101

102 **Figure S11.** Average diurnal profiles along with the standard deviation of PM_{1} species, four OA factors
 103 identified from PMF analysis, various gas-phase species, and meteorological parameters for weekdays (Monday to
 104 Friday inclusive) and weekends (Saturday and Sunday) during the campaign.



105
106 **Figure S12.** (a) Back trajectories of air masses arriving at Handan every hour for 500 m above ground level
107 and four clusters determined using the inbuilt function of HYSPLIT for the entire campaign. The four clusters
108 represent air masses long-range transported from the north (LRN, 23.8%), from the northeast (NE, 30.0%),
109 from the northwest (NW, 18.9%), and long-range transported from the northwest (LRNW, 27.3%). (b) Mass concentrations
110 and (c) mass fractions of aerosol species for each cluster.

111



112

113

Figure S13. The RH-binned bulk composition of submicron aerosols.

114

115 **References**

- 116 Hu, W., Hu, M., Hu, W., Jimenez, J. L., Yuan, B., Chen, W., Wang, M., Wu, Y., Chen, C., Wang, Z.,
117 Peng, J., Zeng, L., and Shao, M.: Chemical composition, sources and aging process of submicron aerosols
118 in Beijing: contrast between summer and winter, *J. Geophys. Res.*, 121, 1955–1977,
119 doi:10.1002/2015JD024020, 2016a.
- 120 Hu, W., Hu, M., Hu, W.-W., Niu, H., Zheng, J., Wu, Y., Chen, W., Chen, C., Li, L., Shao, M., Xie, S.,
121 and Zhang, Y.: Characterization of submicron aerosols influenced by biomass burning at a site in the
122 Sichuan Basin, southwestern China, *Atmos. Chem. Phys.*, 16, 13213–13230, doi:10.5194/acp-16-13213-
123 2016, 2016b.
- 124 Huang, X. F., Xue, L., Tian, X. D., Shao, W. W., Sun, T. L., Gong, Z. H., Ju, W. W., Jiang, B., Hu, M.,
125 and He, L. Y.: Highly time-resolved carbonaceous aerosol characterization in Yangtze River Delta of
126 China: Composition, mixing state and secondary formation, *Atmos. Environ.*, 64, 200–207,
127 doi:10.1016/j.atmosenv.2012.09.059, 2013.
- 128 Ng, N. L., Canagaratna, M. R., Jimenez, J. L., Zhang, Q., Ulbrich, I. M., and Worsnop, D. R.: Real-time
129 methods for estimating organic component mass concentrations from aerosol mass spectrometer data,
130 *Environ. Sci. Technol.*, 45, 910–916, 2011.
- 131 Paatero, P.: User's guide for positive matrix factorization programs PMF2 and PMF3, 2004.
- 132 Sun, Y. L., Wang, Z. F., Fu, P. Q., Yang, T., Jiang, Q., Dong, H. B., Li, J., and Jia, J. J.: Aerosol
133 composition, sources and processes during wintertime in Beijing, China, *Atmos. Chem. Phys.*, 13, 4577–
134 4592, doi:10.5194/acp-13-4577-2013, 2013.
- 135 Sun, Y., Du, W., Fu, P., Wang, Q., Li, J., Ge, X., Zhang, Q., Zhu, C., Ren, L., Xu, W., Zhao, J., Han, T.,
136 Worsnop, D. R., and Wang, Z.: Primary and secondary aerosols in Beijing in winter: sources, variations
137 and processes, *Atmos. Chem. Phys.*, 16, 8309–8329, doi:10.5194/acp-16-8309-2016, 2016.
- 138 Xu, J., Shi, J., Zhang, Q., Ge, X., Canonaco, F., Prévôt, A. S. H., Vonwiller, M., Szidat, S., Ge, J., Ma,
139 J., An, Y., Kang, S., and Qin, D.: Wintertime organic and inorganic aerosols in Lanzhou, China: Sources,
140 processes and comparison with the results during summer, *Atmos. Chem. Phys. Discuss.*,
141 doi:10.5194/acp-2016-278, in review, 2016.
- 142 Zhang, J. K., Sun, Y., Liu, Z. R., Ji, D. S., Hu, B., Liu, Q., and Wang, Y. S.: Characterization of submicron
143 aerosols during a month of serious pollution in Beijing, 2013, *Atmos. Chem. Phys.*, 14, 2887–2903,
144 doi:10.5194/acp-14-2887-2014, 2014.
- 145 Zhang, Y. J., Tang, L., Yu, H., Wang, Z., Sun, Y., Qin, W., Chen, W., Chen, C., Ding, A., Wu, J., Ge, S.,
146 Chen, C., and Zhou, H.-C.: Chemical composition, sources and evolution processes of aerosol at an urban
147 site in Yangtze River Delta, China during wintertime, *Atmos. Environ.*, 123, 339–349,
148 doi:10.1016/j.atmosenv.2015.08.017, 2015.
- 149
- 150